International Journal of Mobile Network Design and Innovation

ISSN online: 1744-2850 - ISSN print: 1744-2869
https://www.inderscience.com/ijmndi

Interference in dynamic TDD: effect of MIMO rank on DoF and transceiver design

Amel Tibhirt, Dirk Slock, Yi Yuan-Wu

DOI: 10.1504/IJMNDI.2023.10058241

Article History:

Received:	26 May 2023
Last revised:	29 May 2023
Accepted:	08 June 2023
Published online:	03 September 2023

Interference in dynamic TDD: effect of MIMO rank on DoF and transceiver design

Amel Tibhirt*

Orange Labs,
Châtillon, 92320, France
Email: amel.tibhirt@orange.com
*Corresponding author

Dirk Slock

Communication Systems Department,
EURECOM,
Biot, 06410, France
Email: dirk.slock@eurecom.fr

Yi Yuan-Wu

Orange Labs,
Châtillon, 92320, France
Email: yi.yuan@orange.com

Abstract: Dynamic time division duplexing (DynTDD) provides greater flexibility than static time division duplexing (TDD) by dynamically adjusting time slot allocation based on communication needs. However, flexibility may be limited by crosslink interference (CLI) from neighboring cells using different transmission directions on partially-overlapping time-frequency resources. To mitigate this interference, coordinated beamforming is critical. This study focuses on zero-forcing (ZF) transmit beamforming at initialisation, with and without water-filling, and the iterative weighted minimum mean-square error (WMMSE) algorithm to maximise the sum rate in a MIMO user equipment to user equipment (UE-to-UE) interference channel (IC). Additionally, the study explores the potential benefits of non-uniform degrees-of-freedom (DoF) at uplink (UL) and/or downlink (DL) UEs, increasing the sum of DoF, resulting in a higher sum rate at high SNR.

Keywords: DynTDD; dynamic time division duplexing; MIMO; multiple input multiple output; CLI; cross link interference; interference alignment; rank deficient; DoF; degree of freedom; beamforming; WMMSE; weighted minimum mean-square error; zero-forcing; water-filling.

Reference to this paper should be made as follows: Tibhirt, A., Slock, D. and Yuan-Wu, Y. (2023) 'Interference in dynamic TDD: effect of MIMO rank on DoF and transceiver design', *Int. J. Mobile Network Design and Innovation*, Vol. 10, No. 4, pp.222–232.

Biographical notes: Amel Tibhirt specialised in electronics and telecommunications at the National Polytechnic School. Her versatile education allowed her to explore networking, embedded systems, and computer science. She earned a Master's degree in Networking and Telecommunications from the University of Paris Saclay. She had an internship at Orange Labs, proposing an algorithm of slicing for URLLC and eMBB in 5G networks. This experience sparked her interest. Pursuing a Doctoral thesis at Orange, she focuses on reducing cross-link interference in dynamic TDD systems. Amel is committed to advancing telecommunications technology.

Dirk Slock (Fellow, IEEE) received his PhD degree in Electrical Engineering from Stanford University in 1989. He is currently a Professor at EURECOM, teaching wireless communications signal processing. He invented semi-blind channel estimation, MIMO-CDD (part of LTE), and contributed to GSM with Single Antenna Interference Cancellation (SAIC). Recent work focuses on (Massive) MIMO, resource allocation, Bayesian learning, and audio source separation. He supervised 40 PhD students, co-founded SigTone in 2000, and Nestwave in 2014. He received Best Student Paper Awards and is a Fellow of EURASIP.

Yi Yuan-Wu received an Engineering degree in Electronics from Huazhong University of Science and Technology, China, in 1982, and a PhD degree in Signal Processing and Telecommunication from Rennes University, France, in 1987. Her early career involved research on digital diffusion to

mobile systems with CCETT, Rennes. Later, she worked with Thomson-LGT on video diffusion networks from 1989 to 1991. Since 1992, she has been with Orange Innovation in Chatillon, France, serving as a Senior Research Expert since 2004. Her expertise includes signal detection, interference broadcast channels, D2D communications, MIMO beamforming, massive MIMO, and more.

This paper is a revised and expanded version of a paper entitled 'Transceiver design in dynamic TDD with reduced-rank MIMO interference channels' presented at *Wireless Telecommunications Symposium*, Boston, MA, USA, 19–21 April, 2023.

1 Introduction

Multiple input multiple output (MIMO) technology is a promising solution for achieving high throughput in wireless communication systems (Goldsmith, 2005). In Downlink (DL) communication, if the transmitter has certain knowledge of the Channel state information (CSI), the system throughput can be maximised. In this study, we focus on dynamic time division duplexing (DynTDD) systems, which have the potential to significantly improve overall resource utilisation (Jayasinghe et al., 2015) and reduce latency (Yang et al., 2017). However, DynTDD also presents new challenges due to the introduction of cross-link interference (CLI), including Downlink to Uplink (DL-to-UL) and Uplink to Downlink (UL-to-DL) interference. Previous studies have mainly focused on resolving the base station (BS)-to-BS interference problem, while interference between user equipment (UE) has been less explored. This is because, during Uplink (UL) transmission, DL-to-UL interference can cause substantial performance degradation, unlike during DL transmission where DynTDD is used in its favour (Rachad et al., 2018). However, as reported in Han et al. (2010), UE-to-UE interference is low for UEs in the centre of the cell region, but very high for UEs at the cell edge. To improve network capacity significantly and ensure network stability, it is necessary to handle UE-to-UE interference of edge UEs. Therefore, concurrent transmission techniques, such as Zero Forcing (ZF), Interference Alignment (IA), and distributed MIMO, have been proposed, in which multiple senders jointly encode signals to multiple receivers so that interference is aligned or canceled, and each receiver can decode its desired information. The feasibility conditions of IA have been analysed in various studies, such as Liu and Yang (2013), González et al. (2014), Razaviyayn et al. (2011), Chen et al. (2020), Negro et al. (2009), Negro et al. (2010) and Jeon et al. (2017). Additionally, (Ko et al., 2018) has mathematically characterised the achievable Degrees of Freedom (DoF) of their proposed distributed interference alignment (DIA) technique for a given number of antennas at the BS/Mobile Station (MS).

The primary contributions of this paper extend beyond the outcomes of the studies conducted in Tibhirt et al. (2021) and Tibhirt et al. (2022a). In this paper, we utilise the non-uniformity of degrees of freedom (DoF) at Downlink (DL) user equipment (UE) and/or at Uplink (UL) UE to enhance the sum of DoF and thereby increase the rate at high signal-to-noise ratio (SNR). We have substantiated our approach with numerical results and sum rate simulations using a complete Dynamic Time Division Duplex (DynTDD) system that employs Zero Forcing (ZF) transmit filters at the DL Base Station (BS) to tackle the intracell interference. For maximising the sum rate, we have implemented an algorithm that employs ZF beamformers at DL and UL UEs in the initialisation stage to eliminate UE-to-UE interference, ZF transmitter at DL BS to eliminate intracell interference between DL UEs, and WMMSE filters in the iterative process. Additionally, we have employed the water-filling technique to enhance the system's performance at low SNR.

2 System model and problem formulation

Let's consider a MIMO system that consists of two cells, with each cell containing one base station (BS). One cell operates in the downlink (DL) mode, while the other cell operates in the uplink (UL) mode. The UL and DL cells are equipped with M_{ul} and M_{dl} antennas, respectively, and there are K_{ul} and K_{dl} interfering or interfered users in the UL and DL cells, respectively. The kth DL user equipment (UE) and the lth UL UE are equipped with $N_{dl,k}$ and $N_{ul,l}$ antennas, respectively. Due to the different configurations in DynTDD between neighbouring cells, two types of interference arise the UE-to-UE interference between the UEs located at the edge of the two cells (as shown in Figure 1), and the BS-to-BS interference. Our system, as shown in Figure 1, is known as interfering broadcast-multiple access channel (IBMAC) in Jeon et al. (2017). It represents a two-cell system, with one cell in DL mode (broadcast) and the other in UL mode (multiple access), with interference between the two cells. For this study, we assume that the number of BS antennas is large enough to support all UL or DL UE streams and that the BS-to-BS interference can be mitigated by utilising a limited rank BS-to-BS channel (Ko et al., 2018). As a result, the IBMAC problem is then limited to interference from UL UEs to DL UEs, which we refer to as IBMAC-IC (IBMAC Interference Channel). In terms of the number of data streams at the transmitter and receiver, we make the following assumptions:

$$d_{dl,k} \geq 1 \quad and \quad d_{ul,l} \geq 1. \tag{1}$$

The lth UL user transmits $d_{ul,l}$ independent streams to the UL BS, where $p_{ul,l}$ represents the non-negative UL power at user l. At the same time, the kth DL user receives $d_{dl,k}$ independent streams from the DL BS, with non-negative DL power allocation $p_{dl,k}$. Let $\boldsymbol{V}_{dl,k} \in \mathbb{C}^{M_{dl} \times d_{dl,k}}$ denote the beamformer used by the DL BS to transmit the signal $s_{dl,k} \in \mathbb{C}^{d_{dl,k}\times 1}$ to the kth DL UE, and $\boldsymbol{V}_{ul,l} \in \mathbb{C}^{N_{ul,l}\times d_{ul,l}}$ denote the beamformer used by the lth UL UE to transmit the signal $s_{ul,l} \in \mathbb{C}^{d_{ul,l}\times 1}$ to the UL BS. We assume that $E[\boldsymbol{s}_{dl,k}\boldsymbol{s}_{dl,k}^H] = \boldsymbol{I}$ and $E[\boldsymbol{s}_{ul,l}\boldsymbol{s}_{ul,l}^H] = \boldsymbol{I}$. Furthermore, we consider $\boldsymbol{U}_{dl,k} \in \mathbb{C}^{N_{dl,k}\times d_{dl,k}}$ and $\boldsymbol{U}_{ul,l} \in \mathbb{C}^{M_{ul}\times d_{ul,l}}$ as the Rx beamforming matrices at the kth DL UE and UL BS (from the lth UL UE), respectively. The received signal at the kth DL UE is given by $\boldsymbol{y}_{dl,k}$:

$$\boldsymbol{y}_{dl,k} = \underbrace{\boldsymbol{H}_k^{DL}\boldsymbol{V}_{dl,k}\boldsymbol{s}_{dl,k}}_{\text{desired signal}} + \underbrace{\sum_{j=1,j\neq k}^{K_{dl}} \boldsymbol{H}_k^{DL}\boldsymbol{V}_{dl,j}\boldsymbol{s}_{dl,j}}_{\text{intracell interference}}$$

$$+ \underbrace{\sum_{l=1}^{K_{ul}} \boldsymbol{H}_{k,l}\boldsymbol{V}_{ul,l}s_{ul,l}}_{\text{UL To DL interference}} + \underbrace{\boldsymbol{n}_{dl,k}}_{\text{noise}}, \tag{2}$$

where the matrix $\boldsymbol{H}_k^{DL} \in \mathbb{C}^{N_{dl,k}\times M_{dl}}$ represents the channel from the DL BS to the kth DL UE. And $H_l^{UL} \in \mathbb{C}^{M_{ul}\times N_{ul,l}}$ in (4) is the matrix of the channel from the lth UL UE to the UL BS. We call $\boldsymbol{H}_k^{DL}$ and $\boldsymbol{H}_l^{UL}$ the direct channels. The interference channel between the $l$thUL and the kth DL UEs is denoted as $H_{k,l} \in \mathbb{C}^{N_{dl,k}\times N_{ul,l}}$. $n_{dl,k} \in \mathbb{C}^{N_{dl,k}\times 1}$ denotes the additive white Gaussian noise with distribution $\mathcal{CN} \in (0,\, \sigma_{dl,k}^2\boldsymbol{I})$ at the kth DL UE. ZF from UL UE l to the DL UE k requires:

$$\boldsymbol{U}_{dl,k}^H\boldsymbol{H}_{k,l}\boldsymbol{V}_{ul,l} = \boldsymbol{0}, \forall k \in \{1,...,K_{dl}\}, \forall l \in \{1,...,K_{ul}\}\,. \tag{3}$$

For this system the achievable rate for the UL user l is given as:

$$\boldsymbol{R}_{ul,l} = \log\det\Bigg(\boldsymbol{I}_{M_{ul}} + \boldsymbol{H}_l^{UL}\boldsymbol{V}_{ul,l}\boldsymbol{V}_{ul,l}^H(\boldsymbol{H}_l^{UL})^H$$

$$\left(\sum_{i=1,i\neq l}^{K_{ul}} \boldsymbol{H}_i^{UL}\boldsymbol{V}_{ul,i}\boldsymbol{V}_{ul,i}^H(\boldsymbol{H}_i^{UL})^H + \sigma_{ul}^2\boldsymbol{I}_{M_{ul}}\right)^{-1}\Bigg). \tag{4}$$

In our study we consider ZF precoders $\boldsymbol{V}_{ul,l}$ at each UL UE given as:

$$\boldsymbol{V}_{ul,l} = \sqrt{\frac{p_{ul,l}}{\mathrm{Tr}(\boldsymbol{G}_{z,l}\boldsymbol{G}_{z,l}^H)}}\boldsymbol{G}_{z,l}. \tag{5}$$

The beamformer at the lth UL UE, denoted by $\boldsymbol{G}_{z,l}$, is obtained by applying the ZF process that satisfies (3). This process is typically iterative, but for certain special cases, it can be obtained in closed-form. Section 5.1 provides a detailed description of the process for obtaining $\boldsymbol{G}_{z,l}$ in such special systems.

The achievable rate for the DL user k is given as:

$$\boldsymbol{R}_{dl,k} = \log\det\Bigg(\boldsymbol{I}_{N_{dl,k}} + \boldsymbol{H}_k^{DL}\boldsymbol{V}_{dl,k}\boldsymbol{V}_{dl,k}^H(\boldsymbol{H}_k^{DL})^H$$

$$\Big(\textstyle\sum_{j=1,j\neq k}^{K_{dl}} \boldsymbol{H}_k^{DL}\boldsymbol{V}_{dl,j}\boldsymbol{V}_{dl,j}^H(\boldsymbol{H}_k^{DL})^H + \tag{6}$$

$$\textstyle\sum_{l=1}^{K_{ul}} \boldsymbol{H}_{k,l}\boldsymbol{V}_{ul,l}\boldsymbol{V}_{ul,l}^H\boldsymbol{H}_{k,l}^H + \sigma_{dl,k}^2\boldsymbol{I}_{N_{dl,k}}\Big)^{-1}\Bigg).$$

In our study we choose $\boldsymbol{V}_{dl,k}$ as ZF transmit filter at the DL BS for the kth DL UE, which is computed as:

$$\boldsymbol{V}_{dl} = b\bar{\boldsymbol{V}} = \left[\boldsymbol{V}_{dl,1}, \boldsymbol{V}_{dl,2}, \ldots, \boldsymbol{V}_{dl,K_{dl}}\right], \tag{7a}$$

$$\bar{\boldsymbol{V}}_{dl} = \boldsymbol{H}^H\boldsymbol{F}\left(\boldsymbol{F}^H\boldsymbol{H}\boldsymbol{H}^H\boldsymbol{F}\right)^{-1}, \tag{7b}$$

$$b = \sqrt{\frac{\sum_{k=1}^{K_{dl}} p_{dl,k}}{\mathrm{Tr}(\bar{\boldsymbol{V}}_{dl}\bar{\boldsymbol{V}}_{dl}^H)}}. \tag{7c}$$

where $\boldsymbol{H} \in \mathbb{C}^{K_{dl}N_{dl,k}\times M_{dl}}$ contains the different DL channel matrices stacked row-wise and $\boldsymbol{F} \in \mathbb{C}^{K_{dl}N_{dl,k}\times K_{dl}d_{dl,k}}$ is blocked diagonal matrix, and are given such that:

$$\boldsymbol{H} = \begin{bmatrix} \boldsymbol{H}_1^{DL} \\ \vdots \\ \boldsymbol{H}_{K_{dl}}^{DL} \end{bmatrix}, \boldsymbol{F} = \begin{bmatrix} \boldsymbol{F}_{z,1} & \boldsymbol{0} & \ldots & \boldsymbol{0} \\ \boldsymbol{0} & \boldsymbol{F}_{z,2} & \ldots & \boldsymbol{0} \\ \vdots & & \ddots & \vdots \\ \boldsymbol{0} & \ldots & \boldsymbol{0} & \boldsymbol{F}_{z,K_{dl}} \end{bmatrix} \tag{8}$$

The beamformer at the kth DL UE, denoted by $\boldsymbol{F}_{z,k}$, is obtained through the ZF process satisfying (3). While this process is iterative in general, it can be in closed-form for some special cases, and the detailed process to obtain $\boldsymbol{F}_{z,k}$ for such a special case is discussed in section 5.1. In the WMMSE study, we sometimes use $\boldsymbol{U}_{dl,k} = \boldsymbol{F}_{z,k}$ to find the initial beams at the DL-BS.

Table 1 presents a summary of the notations used in this paper to facilitate easy reference and understanding.

Figure 1 DynTDD system model (see online version for colours)

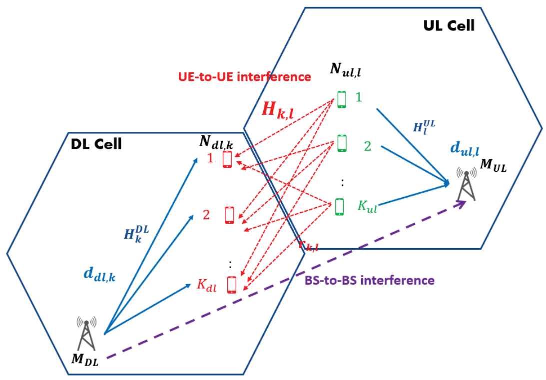

3 IA feasibility conditions for DynTDD UE-to-UE generic Rank MIMO IBMAC

3.1 Proper condition

In Tibhirt et al. (2022a), the proper conditions for IA feasibility in rank deficient MIMO IBMAC-IC were established. The following theorem provides global proper conditions, which typically involve a single global condition that requires the number of variables to be greater than or equal to the number of constraints:

Theorem 1 (Global proper condition for IA feasibility in rank deficient MIMO IBMAC-IC)**:** For rank deficient MIMO channels, if the tuple of DoF $(d_{ul,1}, ..., d_{ul,K_{ul}}, d_{dl,1}, ..., d_{ul,K_{dl}})$ is achievable through IA, then it must satisfy the global proper condition:

$$\begin{aligned}&\textstyle\sum_{l=1}^{K_{ul}} d_{ul,l}(N_{ul,l} - d_{ul,l}) + \sum_{k=1}^{K_{dl}} d_{dl,k}(N_{dl,k} - d_{dl,k}) \\ &\geq \textstyle\sum_{l=1}^{K_{ul}} \sum_{k=1}^{K_{dl}} \min(r_{k,l} d_{dl,k}, r_{k,l} d_{ul,l}, d_{ul,l} d_{dl,k}).\end{aligned} \tag{9}$$

Table 1 Notation

Notation	*References*
$d_{dl,k}$, $d_{ul,l}$	Number of data streams at the kth DL UE, at the lth UL UE respectively
$N_{dl,k}$, $N_{ul,l}$	Number of antennas at the kth DL UE, at the lth UL UE respectively
K_{dl}, K_{ul}	Number of DL UEs, of UL UEs respectively
M_{dl}, M_{ul}	Number of antennas at the DL BS, at the UL BS respectively
$p_{dl,k}$, $p_{ul,l}$	The power at DL BS for the kth DL UE, at the lth UL UE respectively
$s_{dl,k}$, $s_{ul,l}$	Tx signal from DL BS to the kth DL UE, from the lth UL UE respectively
$\boldsymbol{H}_k^{DL}$,$\boldsymbol{H}_l^{UL}$	Direct channel from the DL BS to the kth DL UE, from the lth UL UE to the UL BS respectively
$\boldsymbol{H}_{k,l}$	Interference channel between the lth UL UE and the kth DL UE
$\boldsymbol{V}_{dl,k}$, $\boldsymbol{V}_{ul,l}$	Tx beamforming at the DL BS for the kth DL UE, at the lth UL UE respectively
$\boldsymbol{U}_{dl,k}$, $\boldsymbol{U}_{ul,l}$	Rx beamforming at the kth DL UE, at the UL BS

3.2 Necessary and sufficient condition

The conditions for the feasibility of interference alignment, which involve analysing an IA solution that satisfies equation (3), are elaborated in Tibhirt et al. (2022a). This analysis provides a necessary and sufficient condition for interference alignment feasibility and is described in Theorem 2 for a full-rank interference channel. The condition given by Theorem 2 represents a precise characterisation of the feasibility:

Theorem 2 (Necessary and sufficient condition for IA feasibility in a regular MIMO IBMAC-IC)**:** For a full rank MIMO IBMAC-IC, the DoF tuple $(d_{ul,1}, ..., d_{ul,K_{ul}}, d_{dl,1}, ..., d_{ul,K_{dl}})$ is feasible almost surely if and only if $\boldsymbol{J}$ has full row rank.

$$\boldsymbol{J} = \left[\begin{matrix} \underbrace{\begin{matrix} \boldsymbol{I}_{d_{ul,1}} \otimes \boldsymbol{H}_{11}^{(2)} & \boldsymbol{0} \\ \vdots & \vdots \\ \boldsymbol{0} & \boldsymbol{I}_{d_{ul,K_{ul}}} \otimes \boldsymbol{H}_{1K_{ul}}^{(2)} \\ \vdots & \vdots \\ \boldsymbol{I}_{d_{ul,1}} \otimes \boldsymbol{H}_{K_{dl}1}^{(2)} & \boldsymbol{0} \\ \vdots & \vdots \\ \boldsymbol{0} & \boldsymbol{I}_{d_{ul,K_{ul}}} \otimes \boldsymbol{H}_{K_{dl}K_{ul}}^{(2)} \end{matrix}}_{\boldsymbol{J}_G} & \underbrace{\begin{matrix} (\boldsymbol{H}_{11}^{(3)})^T \otimes \boldsymbol{I}_{d_{dl,1}} & \boldsymbol{0} \\ \vdots & \vdots \\ (\boldsymbol{H}_{1K_{ul}}^{(3)})^T \otimes \boldsymbol{I}_{d_{dl,1}} & \boldsymbol{0} \\ \vdots & \vdots \\ \boldsymbol{0} & (\boldsymbol{H}_{K_{dl}1}^{(3)})^T \otimes \boldsymbol{I}_{d_{dl,K_{dl}}} \\ \vdots & \vdots \\ \boldsymbol{0} & (\boldsymbol{H}_{K_{dl}K_{ul}}^{(3)})^T \otimes \boldsymbol{I}_{d_{dl,K_{dl}}} \end{matrix}}_{\boldsymbol{J}_F} \end{matrix}\right] \tag{10}$$

Such that the matrices $\boldsymbol{H}_{kl}^{(2)} \in \mathbb{C}^{d_{dl,k} \times (N_{ul,l} - d_{ul,l})}$ and $\boldsymbol{H}_{kl}^{(3)} \in \mathbb{C}^{(N_{dl,k} - d_{dl,k}) \times d_{ul,l}}$ correspond to the following channel partitioning:

$$\boldsymbol{H}_{kl} = \begin{bmatrix} \boldsymbol{H}_{kl}^{(1)} \boldsymbol{H}_{kl}^{(2)} \\ \boldsymbol{H}_{kl}^{(3)} \boldsymbol{H}_{kl}^{(4)} \end{bmatrix}. \tag{11}$$

In the case of a reduced-rank interference channel, the UE-to-UE interference channel has a rank of $r_{k,l}$, which means that $r_{k,l}$ distinct significant paths contribute to $\boldsymbol{H}_{k,l}$. As a result, we can decompose $\boldsymbol{H}_{k,l}$ as follows:

$$\boldsymbol{H}_{k,l} = \boldsymbol{B}_{k,l} \boldsymbol{A}_{k,l}^H \tag{12}$$

We define the matrices $\boldsymbol{J}_H$ and $\boldsymbol{J}_J$ such that:

$$\boldsymbol{J}_H = \left[\begin{matrix} \underbrace{\begin{matrix} (\boldsymbol{I}_{d_{ul,1}} \otimes \boldsymbol{B}_{11}^{(1)H}) & \boldsymbol{0} \\ \vdots & \vdots \\ \boldsymbol{0} & (\boldsymbol{I}_{d_{ul,K_{ul}}} \otimes \boldsymbol{B}_{K_{dl}K_{ul}}^{(1)H}) \end{matrix}}_{\boldsymbol{J}_B} & \underbrace{\begin{matrix} (\boldsymbol{A}_{11}^{(1)T} \otimes \boldsymbol{I}_{d_{dl,1}}) & \boldsymbol{0} \\ \vdots & \vdots \\ \boldsymbol{0} & (\boldsymbol{A}_{K_{dl}K_{ul}}^{(1)T} \otimes \boldsymbol{I}_{d_{dl,K_{dl}}}) \end{matrix}}_{\boldsymbol{J}_A} \end{matrix}\right] \tag{13}$$

$$\boldsymbol{J}_J = [\boldsymbol{J} \;\; \boldsymbol{J}_H] \tag{14}$$

Then the necessary and sufficient condition is given by Theorem 3:

Theorem 3 (Necessary and sufficient condition for IA feasibility in reduced rank MIMO IBMAC-IC)**:** For a deficient rank MIMO IBMAC-IC, the DoF $(d_{ul,1}, ..., d_{ul,K_{ul}}, d_{dl,1}, ..., d_{ul,K_{dl}})$ are feasible almost surely if and only if:

$$\text{rank}(\boldsymbol{J}) = \text{rank}(\boldsymbol{J}_J) = \text{rank}([\boldsymbol{J} \;\; \boldsymbol{J}_H]) \tag{15}$$

i.e., the column space of $\boldsymbol{J}_H$ in (13) should be contained in the column space of $\boldsymbol{J}$ in (10).

Detailed proofs of Theorems 2 and 3 can be found in Tibhirt et al. (2022a).

3.3 Sufficient condition

Since Theorems 2 and 3 require the rank of a matrix that includes all the channel matrices, we aimed to find a condition that could be expressed in terms of the system's dimensions, such as $N_{dl,k}$, $N_{ul,l}$, $d_{dl,k}$, $d_{ul,l}$, K_{dl}, and K_{ul}. To achieve this, a sufficient condition is presented in Theorem 4:

Theorem 4 (Sufficient condition for IA feasibility in a regular MIMO IBMAC-IC)**:** For a full rank MIMO IBMAC-IC, respecting the proper condition of Theorem 1, and if:

$$\begin{aligned}&\forall k, l : (N_{ul,l} - d_{ul,l}) \geq d_{dl,k} \;\; \textit{and} \\ &(N_{dl,k} - d_{dl,k}) \geq d_{ul,l}\end{aligned} \tag{16}$$

then $(d_{ul,1}, ..., d_{ul,K_{ul}}, d_{dl,1}, ..., d_{ul,K_{dl}})$ is feasible.

The equation in (16) means that both the block matrix $\boldsymbol{I}_{d_{ul,l}} \otimes \boldsymbol{H}_{kl}^{(2)}$ in $\boldsymbol{J}_G$ and the block matrix $(\boldsymbol{H}_{kl}^{(3)})^T \otimes \boldsymbol{I}_{d_{dl,k}}$ in $\boldsymbol{J}_F$

should be full row rank. The proof is given in Tibhirt et al. (2022b).

We analyse the feasibility of the combined method that is given in (Tibhirt et al., 2021, equations(26), (27)). For this, we compare the DoF given by the combined method in (Tibhirt et al., 2021, equations (26), (27)) to the DoF given by the sufficient and necessary condition for a generic rank interference channel in Theorem 3, which is a precise characterisation of the feasible DoF. And we make our observation in the following conjecture:

Conjecture 1: *For a DynTDD system, if the DoF tuple* $(d_{ul,1},...,d_{ul,K_{ul}},d_{dl,1},...,d_{dl,K_{dl}})$ *satisfies the condition for the combined method in (Tibhirt et al., 2021, eq.(26), eq.(27)), then this DoF is almost surely feasible.*

Then we exploit the non-uniform DoF between DL UEs and between UL UEs, i.e., when the number of the data stream at each DL UE, $d_{dl,k}$, or at each UL UE, $d_{ul,l}$, could be different from each other. As a result, we give the following remark:

Remark 1: In DynTDD systems, if the DoF tuple $(d_{ul,1},...,d_{ul,K_{ul}},d_{dl,1},...,d_{dl,K_{dl}})$ is feasible for IA (i.e., satisfy Theorem 3, and present a non-uniform DoF at Rx (DL UEs) and/or at Tx (UL UEs), so the resulting sum of DoF would be surely equal or greater than the sum DoF when imposing uniform DoF.

Generally speaking, fewer constraints will lead to equal or better performance.

4 Numerical DoF evaluations

To investigate Conjecture 1 and Remark 1, we present Table 2, which considers a MIMO IBMAC-IC and evaluates the DoF of the system for $N_{ul}=3$, $N_{dl}=6$, $K_{ul}=2$, and $K_{dl}=4$. Each element in Table 2 is described below, where a generic tuple (d_{dl},d_{ul},d_{tot}) represents the DoF of a DL UE, a UL UE, and the total UL+DL sum DoF:

- $(d_{p,dl},d_{p,ul},d_{p,tot})$ considering Theorem 1 in the centralised case, i.e., considering (only) the proper (necessary) IA feasibility conditions for a centralised design,
- $(d_{d,dl},d_{d,ul},d_{d,tot})$ considering the distributed method, with DL UE DoF as in (Tibhirt et al., 2021, equation (31a)), UL UE DoF as in (Tibhirt et al., 2021, equation (31b)) (with the corresponding optimised n_F, n_G shown in Table 2 and denoted as n_{F_d}, n_{G_d}), i.e., this is the distributed method in which Tx/Rx filters only depend on the low-rank channel factors on their side (and are independent of the filter values on the other side, their design is closed-form, non-iterative), with an optimisation of the distribution of the ZF roles among Tx/Rx,
- $(d_{c,dl},d_{c,ul},d_{c,tot})$ considering the combined method, with DL UE DoF as in (Tibhirt et al., 2021, equation (26)), the UL UE as in (Tibhirt et al., 2021, equation (27)) (with the corresponding optimised n_F, n_G shown in Table 2 and denoted as n_{F_c}, n_{G_c}), i.e., this concerns a feasible centralised approach in which there is an optimised partitioning of the ZF roles among all Tx/Rx: each interference link is either ZF'd by the Tx or the Rx involved (but the resulting Tx depends on the Rx and vice versa, the Tx/Rx design may require an iterative algorithm),
- $(d_{r,dl},d_{r,ul},d_{r,tot})$ considering Rx side ZF only as in (Tibhirt et al., 2021, equation (26)) with $n_F=K_{ul}$, i.e., all ZF is done by the Rx only (closed-form solutions, non-iterative, hence can be considered a distributed approach),
- $(d_{t,dl},d_{t,ul},d_{t,tot})$ considering Tx side ZF only as in (Tibhirt et al., 2021, equation (27)) with $n_G=K_{dl}$, i.e., all ZF is done by the Tx only (closed-form solutions, non-iterative, hence can be considered a distributed approach),
- $(d_{T3,dl},d_{T3,ul},d_{T3,tot})$ considering Theorem 3, i.e., the exactly maximally feasible DoF in a centralised approach (requires an iterative Tx/Rx design).

For the application of Theorem 3, we perform an algorithm that allows us to check the rank of the matrices $\boldsymbol{J}$ and $\boldsymbol{J}_J$ depending on the variables N_{ul}, N_{dl}, d_{ul}, d_{dl} and r_{kl}, when given the interference channel matrix $\boldsymbol{H}_{k,l}$ with random coefficients that must satisfy the considered rank of the channel matrix.

In Table 2 we can conclude that all the given DoF by the combined method (Tibhirt et al., 2021, equations (26), (27)) is feasible as long as this DoF satisfies the necessary and sufficient condition in Theorem 3. For Remark 1, we can observe, in Table 2 for $r=2$ and when considering the condition in Theorem 3, that the non uniform tuple DoF $d_{ul,1}=d_{ul,2}=1, d_{dl,1}=d_{dl,2}=5, d_{dl,3}=d_{dl,4}=4$, which gives a sum of DoF equal to 20, is feasible. Otherwise, if we assume a uniform DoF (i.e., $d_{ul,1}=d_{ul,2}$ and $d_{dl,1}=d_{dl,2}=d_{dl,3}=d_{dl,4}$) we are limited to a feasible sum of DoF equal to 18. Exploring different numbers of data streams for the Rx and Tx users could be an interesting approach to increase the sum DoF, thereby enhancing the rate performance at high SNR levels.

In Table 3 we compare the number of combinations (a combination is a given number of data streams at each UL and DL UE) for different sum DoF when considering the proper condition in Theorem 1, the necessary and sufficient condition in Theorem 2, the sufficient condition in Theorem 4, and the sufficient condition in (Jeon et al., 2017, Theorem 3). We choose as an example $K_{ul}=2$ and $K_{dl}=3$, for the following three systems:

- *System 1*: $N_{ul,1}=3, N_{ul,2}=7, N_{dl,1}=2, N_{dl,2}=3$ and $N_{dl,3}=8$, which is the system that has been chosen in Jeon et al. (2017)
- *System 2*: $N_{ul,1}=4, N_{ul,2}=7, N_{dl,1}=4, N_{dl,2}=5$ and $N_{dl,3}=6$

Table 2 DoF per user as a function of the rank of any cross-link channel with $N_{ul} = 3$, $N_{dl} = 6$, $K_{ul} = 2$ and $K_{dl} = 4$ (see online version for colours)

r	*0*	*1*	*2*	*3*
($d_{p,dl}$,$d_{p,ul}$,$d_{p,tot}$)	(6,3,30)	((6,5,5,5),2,25)	((6,5,5,5),1,23)	(5,1,22)
($d_{d,dl}$,$d_{d,ul}$,$d_{d,tot}$)	(6,3,30)	(5,1,22)	(2,3,14)or (4,0,16)*	(3,0,12)*
($n_{F,d}$,$n_{G,d}$)	(1,2)	(1,2)	(1,2) or (2,0)	(1,2)
($d_{c,dl}$,$d_{c,ul}$,$d_{c,tot}$)	(6,3,30)	(5,1,22)	(4,1,18)	(4,1,18)
($n_{F,c}$,$n_{G,c}$)	(1,2)	(1,2)	(2,0)	(2,0)
($d_{r,dl}$, $d_{r,ul}$, $d_{r,tot}$)	(6,3,30)	(4,3,18)	(2,3,14)	(0,3,6)*
($d_{t,dl}$, $d_{t,ul}$, $d_{t,tot}$)	(6,3,30)	(6,0,24)*	(6,0,24)*	(6,0,24)*
($d_{T3,dl}$, $d_{T3,ul}$, $d_{T3,tot}$)	(6,3,30)	(5,1,22)	((5,5,4,4),1,20)**	(4,1,18)

(*): the given DoF does not satisfy the conditions in (1) if a negative DoF results from a formula, this DoF will be set to zero logically.
(**): the given DoF represents a non-uniform DoF at DL UEs, of the form $((d_{dl,1}, d_{dl,2}, d_{dl,3}, d_{dl,4}), d_{ul}, d_{tot})$.

- *System 3*: $N_{ul,1} = 7, N_{ul,2} = 7, N_{dl,1} = 6, N_{dl,2} = 5$ and $N_{dl,3} = 6$.

We get the following numerical results by doing an exhaustive search for all the possible combinations that satisfy each given theorem in Table 3, and this process is repeated for different sum DoF. We give here an example to better understand the meaning of a combination, for System 1 when $SumDoF = 6$, the different possible combinations that respect the proper condition in Theorem 1 are:

$$d_{ul,1} = 2, d_{ul,2} = 1, d_{dl,1} = 1, d_{dl,2} = 1 \text{ and } d_{dl,3} = 1$$

$$d_{ul,1} = 1, d_{ul,2} = 2, d_{dl,1} = 1, d_{dl,2} = 1 \text{ and } d_{dl,3} = 1$$

$$d_{ul,1} = 1, d_{ul,2} = 1, d_{dl,1} = 2, d_{dl,2} = 1 \text{ and } d_{dl,3} = 1$$

$$d_{ul,1} = 1, d_{ul,2} = 1, d_{dl,1} = 1, d_{dl,2} = 2 \text{ and } d_{dl,3} = 1$$

$$d_{ul,1} = 1, d_{ul,2} = 1, d_{dl,1} = 1, d_{dl,2} = 1 \text{ and } d_{dl,3} = 2.$$

Table 3 Number of combinations for different Sum DoF in a full rank interference channel, $K_{ul} = 2$ and $K_{dl} = 3$ (see online version for colours)

Sum_{DoF}	5	6	7	8	9	10	11	12	13	14	15
Proper Theorem 1_{SYS1}	1	5	10	15	20	21	19	5	0	0	0
Theorem 2_{SYS1}	1	5	10	15	20	21	16	3	0	0	0
Theorem 4 $(16)_{SYS1}$	1	2	1	0	0	0	0	0	0	0	0
(Jeon et al. 2017, Theorem $3)_{SYS1}$	1	0	0	1	0	0	0	0	0	0	0
Proper Theorem 1_{SYS2}	1	5	15	33	58	83	80	26	4	0	0
Theorem 2_{SYS2}	1	5	15	31	50	67	60	21	4	0	0
Theorem 4 $(16)_{SYS2}$	1	5	15	22	20	9	2	0	0	0	0
(Jeon et al. 2017, Theorem $3)_{SYS2}$	1	0	0	0	0	0	1	0	0	0	0
Proper Theorem 1_{SYS3}	1	5	15	35	70	125	189	241	187	51	8
Theorem 2_{SYS3}	1	5	15	35	70	125	173	197	167	51	8
Theorem 4 $(16)_{SYS3}$	1	5	15	35	61	76	72	52	28	12	3
(Jeon et al. 2017, Theorem $3)_{SYS3}$	1	0	0	1	0	0	1	0	0	0	0

From these results, we can conclude that:

- The gap in terms of the number of combinations between the proper (Theorem 1) and the necessary and sufficient condition (Theorem 2) is not negligible, and it is proportional to the number of antennas. Thus a feasible Sum DoF needs to be associated with feasible combinations (distribution of the DoF at UL and DL UE), so the IA is feasible,
- All the feasible cases are given by the necessary and sufficient condition (Theorem 2), the sufficient condition (Theorem 4) comes to cover a subset of these feasible cases, the size of this subset is quite interesting, since Theorem 4 is written in term of the problem dimension, and does not need the full row rank test on $\boldsymbol{J}$,
- When considering the sufficient condition (Theorem 4) with the sufficient condition mentioned before in the state of the art (Jeon et al., 2017, Theorem 3), we notice how much the sufficient condition in Theorem 4 outperforms and improves the available state of the art.

5 Beamformer design

In this section, we begin by furnishing an example of how to obtain the ZF precoders for UL UEs and the ZF decoders for DL UEs when working with closed-form cases. Furthermore, we introduce the WMMSE beamformer and finally, we describe the algorithm that is used for water-filling.

5.1 *The ZF precoders at UL UEs and the ZF decoders at DL UEs*

In this subsection, we provide an explanation of how we derive the ZF precoders $\boldsymbol{G}_{z,l}$ and the ZF decoders $\boldsymbol{F}_{z,k}$ in closed-form cases, which allow us to satisfy the condition of canceling all interference links from the UL UEs to the DL UEs given in equation (3).

We consider a system with $N_{ul} = 3$, $N_{dl} = 6$, $K_{ul} = 2$, and $K_{dl} = 4$, with an interference channel matrix of rank $r = 2$. We assume that the data stream is $d_{ul,1} = d_{ul,2} = 1, d_{dl,1} = d_{dl,2} = 5$, and $d_{dl,3} = d_{dl,4} = 4$. The following steps illustrate how we obtain $\boldsymbol{G}_{z,l}$ and $\boldsymbol{F}_{z,k}$ in closed-form cases:

Step 0: We generate interference channel matrices $\boldsymbol{H}_{11}, \boldsymbol{H}_{12}, \boldsymbol{H}_{21}, \boldsymbol{H}_{22}, \boldsymbol{H}_{31}, \boldsymbol{H}_{32}, \boldsymbol{H}_{41}$ and $\boldsymbol{H}_{42}$ with a rank of $r = 2$.

Step 1: The stream from UL UE 1 to DL UE 1 is canceled by UL UE 1. This involves performing singular value decomposition (SVD) of the interference channel matrix $\boldsymbol{H}_{11}$, resulting in:

$$\left[\boldsymbol{U}_{t1}\boldsymbol{S}_{t1}\boldsymbol{V}_{t1}\right] = SVD(\boldsymbol{H}_{11}). \tag{17}$$

${\boldsymbol{S}_{t1}}^1$ is given such that:

$$\boldsymbol{S}_{t1} = \begin{bmatrix} 0 & 0 & 0 \\ 0 & \beta_{1,1} & 0 \\ 0 & 0 & \beta_{1,2} \\ 0 & 0 & 0 \\ 0 & 0 & 0 \\ 0 & 0 & 0 \end{bmatrix} \tag{18}$$

After obtaining the SVD of the interference channel matrix $\boldsymbol{H}_{11}$ and denoting the non-zero singular values by $\beta_{1,1}$ and $\beta_{1,2}$, we set $\boldsymbol{V}_{N1} = \boldsymbol{V}_{t1}$ and use it to transmit from Tx 1 (UL UE 1). This results in the following updated interference channel matrices:

$$\boldsymbol{H}_{N1,k1} = \boldsymbol{H}_{k1}\boldsymbol{V}_{N1}, \forall k \in [1, ..., K_{dl}] \tag{19}$$

The resulting $\boldsymbol{H}_{N1,11}$ has zeros at the first column, thus the interference from the UL UE 1 to the DL UE 1 is canceled by the UL UE 1.

Step 2: we perform interference cancellation from UL UE 2 to DL UE 2. This is achieved by performing the SVD of the interference channel matrix $\boldsymbol{H}_{22}$, which yields:

$$\left[\boldsymbol{U}_{t2}\boldsymbol{S}_{t2}\boldsymbol{V}_{t2}\right] = SVD(\boldsymbol{H}_{22}). \tag{20}$$

where the positions of the two non-zero singular values of $\boldsymbol{S}_{t2}$ are as those of $\boldsymbol{S}_{t1}$.

Then we take $\boldsymbol{V}_{N2} = \boldsymbol{V}_{t2}$ and apply it to Tx 2 (UL UE 2), so the new interference channel matrices become:

$$\boldsymbol{H}_{N2,k2} = \boldsymbol{H}_{k2}\boldsymbol{V}_{N2}, \forall k \in [1, ..., K_{dl}] \tag{21}$$

The resulting $\boldsymbol{H}_{N2,22}$ has zeros at the first column, thus the interference from the UL UE 2 to the DL UE 2 is canceled by UL UE 2.

Step 3: To cancel the stream from UL UE 2 to DL UE 1, we obtain the new channel matrix $\boldsymbol{H}_{N2,12}$ after completing step 2. Then, we calculate the SVD of the first column of $\boldsymbol{H}_{N2,12}$, denoted as $\boldsymbol{H}_{N2p,12}$. This step allows us to remove the interference caused by UL UE 2 on DL UE 1:

$$\left[\boldsymbol{U}_1\boldsymbol{S}_1\boldsymbol{V}_1\right] = SVD(\boldsymbol{H}_{N2p,12}). \tag{22}$$

Then we take $\boldsymbol{U}_1^H$ and apply it to Rx 1 (DL UE 1), so the new interference channel matrices become:

$$\boldsymbol{H}_{n1,1l} = \boldsymbol{U}_1^H\boldsymbol{H}_{Nl,1l}, \forall l \in [1, ..., K_{ul}] \tag{23}$$

${\boldsymbol{S}_1}^1$ is given such that:

$$\boldsymbol{S}_1 = \left[0\,0\,0\,0\,0\,\gamma_1\right]^T \tag{24}$$

with γ_1 is the non-zero singular value of $\boldsymbol{H}_{N2p,12}$.
The resulting $\boldsymbol{H}_{n1,12}$ has $d_{dl,1}$ zeros at the first column, thus the interference from the UL UE 2 to the DL UE 1 is canceled at the DL UE 1.

Step 4: To cancel the stream from UL UE 1 to DL UE 2, we use the new channel matrix from UL UE 1 to DL UE 2 obtained after step 1, denoted by $\boldsymbol{H}_{N1,21}$. Then, we consider the first column of $\boldsymbol{H}_{N1,21}$, which corresponds to the stream from UL UE 1 to DL UE 2, denoted by $\boldsymbol{H}_{N1p,21}$. We apply the SVD to $\boldsymbol{H}_{N1p,21}$:

$$\left[\boldsymbol{U}_2\boldsymbol{S}_2\boldsymbol{V}_2\right] = SVD(\boldsymbol{H}_{N1p,21}). \tag{25}$$

where the positions of the non-zero singular value of $\boldsymbol{S}_2$ is as that of $\boldsymbol{S}_1$.
Then we take $\boldsymbol{U}_2^H$ and apply it to Rx 2 (DL UE 2), so the new interference channel matrices become:

$$\boldsymbol{H}_{n2,2l} = \boldsymbol{U}_2^H\boldsymbol{H}_{Nl,2l}, \forall l \in [1, ..., K_{ul}] \tag{26}$$

The resulting $\boldsymbol{H}_{n2,21}$ has $d_{dl,2}$ zeros at the first column, thus the interference from the UL UE 1 to the DL UE 2 is canceled at the DL UE 2.

Step 5: we address the interference coming from both UL UE 1 and UL UE 2 towards DL UE 3. To cancel these two streams, we perform the singular value decomposition (SVD) of the matrix $\boldsymbol{H}_{c,3}$ which is formed by concatenating the interference channels from UL UE 1 and UL UE 2 to DL UE 3:

$$\boldsymbol{H}_{c,3} = \begin{bmatrix} h^{11}_{N1,31} & h^{21}_{N1,31} & h^{31}_{N1,31} & h^{41}_{N1,31} & h^{51}_{N1,31} & h^{61}_{N1,31} \\ h^{11}_{N2,32} & h^{21}_{N2,32} & h^{31}_{N2,32} & h^{41}_{N2,32} & h^{51}_{N2,32} & h^{61}_{N2,32} \end{bmatrix}^T \tag{27}$$

such that $h^{ji}_{N1,31}$ represents the element of $\boldsymbol{H}_{N1,31}$ at the ith column and the jth line:

$$\left[\boldsymbol{U}_3\boldsymbol{S}_3\boldsymbol{V}_3\right] = SVD(\boldsymbol{H}_{c,3}) \tag{28}$$

${\boldsymbol{S}_3}^1$ is given such that:

$$\boldsymbol{S}_3 = \begin{bmatrix} 0\,0\,0\,0 & \gamma_{3,1} & 0 \\ 0\,0\,0\,0 & 0 & \gamma_{3,2} \end{bmatrix}^T \tag{29}$$

with $\gamma_{3,1}$ and $\gamma_{3,2}$ are the non-zero singular values of $\boldsymbol{H}_{c,3}$.
Then we take $\boldsymbol{U}_3^H$ and apply it to Rx 3 (DL UE 3), so the new interference channel matrices become:

$$\boldsymbol{H}_{n3,3l} = \boldsymbol{U}_3^H\boldsymbol{H}_{Nl,3l}, \forall l \in [1, ..., K_{ul}] \tag{30}$$

After applying the cancelation schemes in Steps 1-4, the resulting interference channel matrices $\boldsymbol{H}_{n3,31}$ and $\boldsymbol{H}_{n3,32}$ have a total of $d_{dl,3}$ zeros at the first column. As a result, the interference from UL UE 1 and UL UE 2 to the DL UE 3 are effectively canceled at the DL UE 3.

Step 6: we aim to cancel the interference from UL UE 1 and UL UE 2 at DL UE 4. To achieve this, we follow a similar approach as in Step 5 by considering the SVD of a matrix denoted as $\boldsymbol{H}_{c,4}$ which is similar to $\boldsymbol{H}_{c,3}$ with considering $\boldsymbol{H}_{N1,41}$ and $\boldsymbol{H}_{N2,42}$:

$$\left[\boldsymbol{U}_4\boldsymbol{S}_4\boldsymbol{V}_4\right] = SVD(\boldsymbol{H}_{c,4}). \tag{31}$$

After obtaining the SVD of the matrix $\boldsymbol{H}_{c,4}$ in the previous step, we place the two non-zero singular values of $\boldsymbol{S}_4$ in the same positions as those of $\boldsymbol{S}_3$. Then, we apply the Hermitian transpose of $\boldsymbol{U}_4$ to the received signal at DL UE 4, denoted as Rx 4. Consequently, the interference channel matrices are updated as follows:

$$\boldsymbol{H}_{n4,4l} = \boldsymbol{U}_4^H \boldsymbol{H}_{Nl,4l}, \forall l \in [1, ..., K_{ul}] \tag{32}$$

The resulting $\boldsymbol{H}_{n4,41}$ and $\boldsymbol{H}_{n4,42}$ have $d_{dl,4}$ zeros at the first column, thus the interference from the UL UE 1 and from UL UE 2 to the DL UE 4 are canceled at the DL UE 4.

Finally, $\boldsymbol{F}_{z,1} = \boldsymbol{U}_1[:, 1 : d_{dl,1}]$, $\boldsymbol{F}_{z,2} = \boldsymbol{U}_2[:, 1 : d_{dl,2}]$, $\boldsymbol{F}_{z,3} = \boldsymbol{U}_3[:, 1 : d_{dl,3}]$ and $\boldsymbol{F}_{z,4} = \boldsymbol{U}_4[:, 1 : d_{dl,4}]$; $\boldsymbol{G}_{z,1} = \boldsymbol{V}_{N1}[:, 1 : d_{ul,1}]$ and $\boldsymbol{G}_{z,2} = \boldsymbol{V}_{N2}[:, 1 : d_{ul,2}]$.

5.2 WMMSE Beamformers

The derivation of the WMMSE beamformer for a MIMO Broadcast Channel system is provided previously in Christensen et al. (2008) and Shi et al. (2011). In our study, we have leveraged the WMMSE filter framework proposed in Christensen et al. (2008) and have extended it to account for the unique characteristics of the Dynamic time division duplexing (TDD) system. This allowed us to derive optimised beamformers at DL $\boldsymbol{V}_{dl,1}$ ... $\boldsymbol{V}_{dl,K_{dl}}, \boldsymbol{U}_{dl,1}$ ... $\boldsymbol{U}_{dl,K_{dl}}$ and at UL $\boldsymbol{V}_{ul,1}$ ... $\boldsymbol{V}_{ul,K_{ul}}, \boldsymbol{U}_{ul,1}$ ... $\boldsymbol{U}_{ul,K_{ul}}$ which maximise the weighted sum rate. The maximisation problem can be written at the DL as:

$$\begin{aligned} &\max_{\boldsymbol{v}} \textstyle\sum_{k=1}^{K_{dl}} \alpha_k \boldsymbol{R}_{dl,k} \\ &s.t. \textstyle\sum_{k=1}^{K_{dl}} \mathrm{Tr}(\boldsymbol{V}_{dl,k}\boldsymbol{V}_{dl,k}^H) \leq P_{DL-BS} \end{aligned} \tag{33}$$

with α_k defines the priority for the DL user k in the system, P_{DL-BS} is the power budget at the DL BS, and $\boldsymbol{R}_{dl,k}$ is the rate of user k which is written as shown in equation (6).

The MSE-matrix for user k given that the MMSE-receive filter is applied can be written as:

$$\begin{aligned} &\boldsymbol{E}_{dl,k} = (\boldsymbol{I}_{d_{dl}} - \boldsymbol{U}_{dl,k}^H \boldsymbol{H}_k^{DL} \boldsymbol{V}_{dl,k}) \\ &(\boldsymbol{I}_{d_{dl}} - \boldsymbol{U}_{dl,k}^H \boldsymbol{H}_k^{DL} \boldsymbol{V}_{dl,k})^H \\ &+ \textstyle\sum_{j=1, j\neq k}^{K_{dl}} \boldsymbol{U}_{dl,k} \boldsymbol{H}_k^{DL} \boldsymbol{V}_{dl,j} \boldsymbol{V}_{dl,j}^H (\boldsymbol{H}_k^{DL})^H \boldsymbol{U}_{dl,k}^H \\ &+ \textstyle\sum_{l=1}^{K_{ul}} \boldsymbol{U}_{dl,k} \boldsymbol{H}_{k,l} \boldsymbol{G}_l \boldsymbol{G}_l^H \boldsymbol{H}_{k,l}^H \boldsymbol{U}_{dl,k}^H \\ &\quad + \sigma_k^2 \boldsymbol{U}_{dl,k}^H \boldsymbol{U}_{dl,k}, \end{aligned} \tag{34}$$

So the MMSE receive filter at user k is given as:

$$\boldsymbol{U}_{dl,k}^{MMSE} = \boldsymbol{J}_{dl,k}^{-1} \boldsymbol{H}_k^{DL} \boldsymbol{V}_{dl,k} \tag{35}$$

with:

$$\begin{aligned} &\boldsymbol{J}_{dl,k} = \textstyle\sum_{j=1}^{K_{dl}} \boldsymbol{H}_k^{DL} \boldsymbol{V}_{dl,j} \boldsymbol{V}_{dl,j}^H (\boldsymbol{H}_k^{DL})^H \\ &+ \textstyle\sum_{l=1}^{K_{ul}} \boldsymbol{H}_{k,l} \boldsymbol{V}_{ul,l} \boldsymbol{V}_{ul,l}^H \boldsymbol{H}_{k,l}^H + \sigma_{dl,k}^2 \boldsymbol{I}_{N_{dl,k}} \end{aligned} \tag{36}$$

Using this MMSE receiver, the corresponding MSE matrix is given by:

$$\boldsymbol{E}_{dl,k}^{mmse} = \boldsymbol{I}_{d_{dl,k}} - \boldsymbol{V}_{dl,k}^H (\boldsymbol{H}_k^{Dl})^H \boldsymbol{J}_{dl,k}^{-1} \boldsymbol{H}_k^{DL} \boldsymbol{V}_{dl,k} \tag{37}$$

We denote $\boldsymbol{W}_{dl,k}$ as a constant weight matrix associated with user k, such that:

$$\boldsymbol{W}_{dl,k} = \boldsymbol{E}_{dl,k}^{mmse^{-1}} \tag{38}$$

The precoder at DL user k is given such that:

$$\bar{\boldsymbol{V}}_{dl} = \left(\boldsymbol{H}^H \boldsymbol{U} \boldsymbol{W} \boldsymbol{U}^H \boldsymbol{H} + \mu_{dl} \boldsymbol{I}_{M_{dl}} \right)^{-1} \boldsymbol{H}^H \boldsymbol{U} \boldsymbol{W} \tag{39a}$$

$$b_{dl} = \sqrt{\frac{P_{DL-BS}}{\mathrm{Tr}(\bar{\boldsymbol{V}}_{dl} \bar{\boldsymbol{V}}_{dl}^H)}} \tag{39b}$$

$$\boldsymbol{V}_{dl}^{WMMSE} = b_{dl} \bar{\boldsymbol{V}}_{dl} = \left[\boldsymbol{V}_{dl,1}, \boldsymbol{V}_{dl,2}, ..., \boldsymbol{V}_{dl,K_{dl}}\right] \tag{39c}$$

with μ_{dl} a regularisation parameter given by:

$$\mu_{dl} = \frac{\mathrm{Tr}\left(\boldsymbol{W} \boldsymbol{U}^H \boldsymbol{U} \right)}{P_{DL-BS}} \tag{40}$$

The same approach used to obtain the WMMSE DL beamformers is applicable to derive the UL beamformers as well. Then at UL, the maximisation of the sum rate is given by:

$$\begin{aligned} &\max_{\boldsymbol{v}} \boldsymbol{R}_{ul,l} \\ &s.t. \mathrm{Tr}(\boldsymbol{V}_{ul,l} \boldsymbol{V}_{ul,l}^H) \leq P_{ul,l} \end{aligned} \tag{41}$$

$P_{ul,l}$ is the power budget at the lth UL UE, and $\boldsymbol{R}_{ul,l}$ is the rate of user l which is written as shown in (4). The MMSE receiver at the UL BS:

$$\boldsymbol{U}_{ul,l}^{MMSE} = \boldsymbol{J}_{ul,l}^{-1} \boldsymbol{H}_l^{UL} \boldsymbol{V}_{ul,l} \tag{42}$$

with $\boldsymbol{J}_{ul,l}$ such that:

$$\boldsymbol{J}_{ul,l} = \sum_{i=1}^{K_{ul}} \boldsymbol{H}_i^{UL} \boldsymbol{V}_{ul,i} \boldsymbol{V}_{ul,i}^H (\boldsymbol{H}_i^{UL})^H + \sigma_{ul}^2 \boldsymbol{I}_{M_{ul}} \tag{43}$$

And the MSE matrix is given by:

$$\boldsymbol{E}_{ul,l}^{mmse} = \boldsymbol{I}_{d_{ul,l}} - \boldsymbol{V}_{ul,l}^H (\boldsymbol{H}_l^{Ul})^H \boldsymbol{J}_{ul,l}^{-1} \boldsymbol{H}_l^{UL} \boldsymbol{V}_{ul,l} \tag{44}$$

with the weighted matrix $\boldsymbol{W}_{ul,l}$:

$$\boldsymbol{W}_{ul,l} = \boldsymbol{E}_{ul,l}^{mmse^{-1}} \tag{45}$$

So the precoder at the lth UL user is:

$$\begin{aligned} &\bar{\boldsymbol{V}}_{ul,l} = \Big((\boldsymbol{H}_l^{UL})^H \boldsymbol{U}_{ul,l} \boldsymbol{W}_{ul,l} \boldsymbol{U}_{ul,l}^H \boldsymbol{H}_l^{UL} + \\ &\textstyle\sum_{i=1}^{K_{dl}} (\boldsymbol{H}_{i,l})^H \boldsymbol{U}_{dl,i} \boldsymbol{W}_{dl,i} \boldsymbol{U}_{dl,i}^H \boldsymbol{H}_{i,l} + \mu_{ul,l} \boldsymbol{I}_{N_{ul,l}} \Big)^{-1} \\ &(\boldsymbol{H}_l^{UL})^H \boldsymbol{U}_{ul,l} \boldsymbol{W}_{ul,l} \end{aligned} \tag{46a}$$

$$b_{ul,l} = \sqrt{\frac{P_{ul,l}}{\mathrm{Tr}(\bar{\boldsymbol{V}}_{ul,l} \bar{\boldsymbol{V}}_{ul,l}^H)}} \tag{46b}$$

$$\boldsymbol{V}_{ul,l}^{WMMSE} = b_{ul,l} \bar{\boldsymbol{V}}_{ul,l} \tag{46c}$$

with $\mu_{ul,l}$ a regularisation parameter given by:

$$\mu_{ul,l} = \frac{\mathrm{Tr}\left(\boldsymbol{W}_{ul,l} \boldsymbol{U}_{ul,l}^H \boldsymbol{U}_{ul,l} \right)}{P_{ul,l}} \tag{47}$$

5.3 Waterfilling algorithm

The subsequent section presents a method for applying the MIMO water-filling algorithm to broadband channels. The total rate at the DL, which takes into account the ZF between UL and DL UEs, as well as the ZF between the DL BS and DL UEs, can be expressed as:

$$\begin{aligned}\boldsymbol{R}_{dl} &= \sum_{k=1}^{K_{dl}} \log\det\Bigg(\boldsymbol{I}_{N_{dl,k}} + \tfrac{1}{\sigma_n^2}(\boldsymbol{F}_{z,k}^H\boldsymbol{F}_{z,k})^{-1}\\ &\Big(\boldsymbol{F}_{z,k}^H\boldsymbol{H}_k^{DL}\boldsymbol{V}_{dl,k}\boldsymbol{Q}_{dl,k}\boldsymbol{V}_{dl,k}^H(\boldsymbol{H}_k^{DL})^H\boldsymbol{F}_{z,k}\Big)\Bigg)\\ &= \sum_{k=1}^{K_{dl}} \log\det\Bigg(\boldsymbol{I}_{N_{dl,k}} + \tfrac{1}{\sigma_n^2}\Big(\boldsymbol{V}_{dl,k}^H(\boldsymbol{H}_k^{DL})^H\boldsymbol{F}_{z,k}\\ &(\boldsymbol{F}_{z,k}^H\boldsymbol{F}_{z,k})^{-1}\boldsymbol{F}_{z,k}^H\boldsymbol{H}_k^{DL}\boldsymbol{V}_{dl,k}\boldsymbol{Q}_{dl,k}\Big)\Bigg),\end{aligned} \tag{48}$$

with $\boldsymbol{Q}_{dl,k} = \boldsymbol{I}_{d_{dl,k}}$, and the DL transmit power constraint is $\sum_{k=1}^{K_{dl}} \mathrm{Tr}(\boldsymbol{Q}_{dl,k}\boldsymbol{V}_{dl,k}^H\boldsymbol{V}_{dl,k}) = P$, P is the power budget available at the DL BS.

Now, we consider the eigendecomposition of $\boldsymbol{V}_{dl,k}^H\boldsymbol{V}_{dl,k}$ given by:

$$\boldsymbol{V}_{dl,k}^H\boldsymbol{V}_{dl,k} = \tilde{\boldsymbol{X}}_{dl,k}\tilde{\boldsymbol{\Sigma}}_{dl,k}\tilde{\boldsymbol{X}}_{dl,k}^H \tag{49}$$

where $\tilde{\boldsymbol{X}}_{dl,k}\tilde{\boldsymbol{X}}_{dl,k}^H = \tilde{\boldsymbol{X}}_{dl,k}^H\tilde{\boldsymbol{X}}_{dl,k} = \boldsymbol{I}$, and $\tilde{\boldsymbol{\Sigma}}_{dl,k} = \tilde{\boldsymbol{\Sigma}}_{dl,k}^{1/2}\tilde{\boldsymbol{\Sigma}}_{dl,k}^{1/2}$ is a positive diagonal matrix. Let $\boldsymbol{Q}_{dl,k}^{'} = \tilde{\boldsymbol{\Sigma}}_{dl,k}^{1/2}\tilde{\boldsymbol{X}}_{dl,k}^H\boldsymbol{Q}_{dl,k}\tilde{\boldsymbol{X}}_{dl,k}\tilde{\boldsymbol{\Sigma}}_{dl,k}^{1/2}$ and $\boldsymbol{V}_{dl,k}^{'} = \boldsymbol{V}_{dl,k}\tilde{\boldsymbol{X}}_{dl,k}\tilde{\boldsymbol{\Sigma}}_{dl,k}^{-1/2}$. So with $\boldsymbol{Q}_{dl,k}^{'}$ and $\boldsymbol{V}_{dl,k}^{'}$ (48) could be written such that:

$$\begin{aligned}\boldsymbol{R}_{dl} &= \sum_{k=1}^{K_{dl}} \log\det\Bigg(\boldsymbol{I}_{N_{dl,k}} + \tfrac{1}{\sigma_n^2}\big(\boldsymbol{V}_{dl,k}^{'H}(\boldsymbol{H}_k^{DL})^H\\ &\boldsymbol{F}_{z,k}(\boldsymbol{F}_{z,k}^H\boldsymbol{F}_{z,k})^{-1}\boldsymbol{F}_{z,k}^H\boldsymbol{H}_k^{DL}\boldsymbol{V}_{dl,k}^{'}\boldsymbol{Q}_{dl,k}^{'}\big)\Bigg),\end{aligned} \tag{50}$$

with the DL transmit power constraint $\sum_{k=1}^{K_{dl}} \mathrm{Tr}(\boldsymbol{Q}_{dl,k}^{'}) = P$.

Then, we consider the following eigendecomposition:

$$\begin{aligned}&\tfrac{1}{\sigma_n^2}\boldsymbol{V}_{dl,k}^{'H}(\boldsymbol{H}_k^{DL})^H\boldsymbol{F}_{z,k}(\boldsymbol{F}_{z,k}^H\boldsymbol{F}_{z,k})^{-1}\boldsymbol{F}_{z,k}^H\boldsymbol{H}_k^{DL}\boldsymbol{V}_{dl,k}^{'}\\ &= \boldsymbol{X}_{dl,k}\boldsymbol{\Sigma}_{dl,k}\boldsymbol{X}_{dl,k}^H.\end{aligned} \tag{51}$$

where $\boldsymbol{X}_{dl,k}\boldsymbol{X}_{dl,k}^H = \boldsymbol{X}_{dl,k}^H\boldsymbol{X}_{dl,k} = \boldsymbol{I}$, and $\boldsymbol{\Sigma}_{dl,k} = \boldsymbol{\Sigma}_{dl,k}^{1/2}\boldsymbol{\Sigma}_{dl,k}^{1/2}$ is a positive diagonal matrix. We note $\boldsymbol{V}_{dl,k}^{''} = \boldsymbol{V}_{dl,k}^{'}\boldsymbol{X}_{dl,k}$ and $\boldsymbol{Q}_{dl,k}^{''} = \boldsymbol{X}_{dl,k}^H\boldsymbol{Q}_{dl,k}^{'}\boldsymbol{X}_{dl,k}$, then $\boldsymbol{V}_{dl,k}^{'}\boldsymbol{Q}_{dl,k}^{'}\boldsymbol{V}_{dl,k}^{'H} = \boldsymbol{V}_{dl,k}^{''}\boldsymbol{Q}_{dl,k}^{''}\boldsymbol{V}_{dl,k}^{''H}$.

So the sum rate at DL in (50) becomes:

$$\begin{aligned}\boldsymbol{R}_{dl} &= \sum_{k=1}^{K_{dl}} \log\det\Big(\boldsymbol{I}_{N_{dl,k}} + \tfrac{1}{\sigma_n^2}\big(\boldsymbol{V}_{dl,k}^{"H}(\boldsymbol{H}_k^{DL})^H\\ &\boldsymbol{F}_{z,k}(\boldsymbol{F}_{z,k}^H\boldsymbol{F}_{z,k})^{-1}\boldsymbol{F}_{z,k}^H\boldsymbol{H}_k^{DL}\boldsymbol{V}_{dl,k}^{"}\boldsymbol{Q}_{dl,k}^{"}\big)\Big)\\ &= \sum_{k=1}^{K_{dl}} \log\det\big(\boldsymbol{I}_{N_{dl,k}} + \boldsymbol{\Sigma}_{dl,k}\boldsymbol{Q}_{dl,k}^{"}\big),\end{aligned} \tag{52}$$

The constraint on the transmit power for DL becomes
$\sum_{k=1}^{K_{dl}} \mathrm{Tr}(\boldsymbol{Q}_{dl,k}^{''}) = \sum_{k=1}^{K_{dl}} \mathrm{Tr}(\boldsymbol{Q}_{dl,k}^{'}\boldsymbol{X}_{dl,k}\boldsymbol{X}_{dl,k}^H) = \sum_{k=1}^{K_{dl}} \mathrm{Tr}(\boldsymbol{Q}_{dl,k}^{'}) = P$.

Here, we have $\boldsymbol{Q}_{dl,k}^{''} = diag\{p_{k,1},\ldots,p_{k,d_{dl,k}}\}$ and $\boldsymbol{\Sigma}_{dl,k} = diag\{\sigma_{k,1},\ldots,\sigma_{k,d_{dl,k}}$, represents the power allocated to the kth DL UE at the antennas with the ith data stream. Therefore, the expression for (52) is:

$$\boldsymbol{R}_{dl} = \sum_{k=1}^{K_{dl}}\sum_{i=1}^{d_{dl,k}} \log(1+\sigma_{k,i}p_{k,i}). \tag{53}$$

with the power constraint $\sum_{k=1}^{K_{dl}}\sum_{i=1}^{d_{dl,k}} p_{k,i} = P$. We use the Kuhn-Tucker conditions to verify that the solution $\sum_{k=1}^{K_{dl}}\sum_{i=1}^{d_{dl,k}} p_{k,i} = \sum_{k=1}^{K_{dl}}\sum_{i=1}^{d_{dl,k}} \left[\lambda - \frac{1}{\sigma_{k,i}}\right]_+ = P$ is the assignment that maximises the sum rate, where the optimal λ can be solved using bisection method. In section 6, the P mentioned here will be denoted as P_{DL-BS}.

6 Sum rate simulations

In this section, we evaluate the sum rate of both DL and UL UEs across various scenarios that consider the rank of the MIMO IBMAC-IC and the beamformers implemented.

We start by evaluating the sum rate for the system $N_{ul} = 3, N_{dl} = 6, K_{ul} = 2, K_{dl} = 4, M_{dl} = 20$ and $M_{ul} = 4$. For this, we consider several cases of initialisation of the beamformers and repeat the WMMSE algorithm in an iterative process to maximise the sum rate. In the following, we describe the meaning of each notation associated with a given simulation:

- **init (UE2UE ZF + BS2UE ZF)**: The simulation calculates the sum rate during initialisation with UE-to-UE ZF by utilising UL UEs' precoders $\boldsymbol{G}_{z,l}$ and DL UEs' decoders $\boldsymbol{F}_{z,k}$, and the ZF precoders at the DL BS from (7) to consider the ZF between DL UEs,
- **init (UE EigR + BS2UE ZF)**: The simulation calculates the sum rate during initialisation without UE-to-UE ZF by using UL UEs' precoders and DL UEs' decoders as the reception vectors obtained from the SVD of the direct channel matrices at the UL and DL sides, and the ZF precoders at the DL BS from (7) to consider the ZF between DL UEs,
- **init (UE2UE ZF + BS2UE ZF+ WF)**: The simulation is similar to the **init (UE2UE ZF + BS2UE ZF)** simulation but includes the water-filling algorithm discussed in subsection 5.3,
- **init (UE2UE ZF + BS2UE ZF)+ WMMSE, iter=n**: This simulation starts with the initialisation explained in the **init (UE2UE ZF + BS2UE ZF)** simulation, followed by running the WMMSE algorithm described in section5.2, and returns the sum rate at the nth iteration of the WMMSE algorithm,
- **init (UE EigR + BS2UE ZF)+ WMMSE, iter=n**: This simulation starts with the initialisation explained in the **init (UE EigR + BS2UE ZF)** simulation, followed by running the WMMSE algorithm described in section5.2, and returns the sum rate at the nth iteration of the WMMSE algorithm,

- **init (UE2UE ZF + BS2UE ZF+ WF)+ WMMSE, iter=n**: This simulation starts with the initialisation explained in the **init (UE2UE ZF + BS2UE ZF+ WF)** simulation, followed by running the WMMSE algorithm described in section5.2, and returns the sum rate at the nth iteration of the WMMSE algorithm.

By Monte Carlo averaging over 100 channel realisations, we compute the sum rate at the DL and UL with $\boldsymbol{R}_{dl,k}$ of equation (6) and $\boldsymbol{R}_{ul,l}$ of equation (4), respectively. The direct channel matrices' elements are generated as i.i.d. Gaussian random variables $\mathcal{CN}(0,1)$, and the receive noise covariance is normalised such that $\boldsymbol{R}_{n_k n_k} = \boldsymbol{I}_{N_{dl,k}}$. In simulations without water-filling, we assume the same power at each UL UE, i.e., $P_{ul,1} = P_{ul,2} = P$, and a total power of $K_{dl}P$ at the DL BS, where $\sum_{k=1}^{K_{dl}} p_{dl,k} = K_{dl}P = P_{DL-BS}$ and $P = 10^{\frac{SNR}{10}}$.

In Figure 2, we present the sum rate at the DL and UL UEs for the system with $N_{ul} = 3$, $N_{dl} = 6$, $K_{ul} = 2$, $K_{dl} = 4$, $M_{dl} = 20$, and $M_{ul} = 4$. We consider two cases for the interference channel rank between the UL UEs and the DL UEs, i.e., $rank(\boldsymbol{H}_{k,l}) = r$:

- *Reduced rank MIMO IBMAC-IC*: $r = 2$ such that the DoF at each UL and DL UE is: $d_{ul,1} = d_{ul,2} = 1$ and $d_{dl,1} = d_{dl,2} = 5, d_{dl,3} = d_{dl,4} = 4$. The procedure for acquiring $\boldsymbol{G}_{z,l}$ and $\boldsymbol{F}_{z,k}$ is outlined in subsection 5.1,
- *Full rank MIMO IBMAC-IC*: $r = 3$ such that the DoF at each UL and DL UE is $d_{ul,1} = d_{ul,2} = 1$ and $d_{dl,1} = d_{dl,2} = d_{dl,3} = d_{dl,4} = 4$. As concerning the $\boldsymbol{G}_{z,l}$ and $\boldsymbol{F}_{z,k}$ for $r = 3$, the maximum eigenvector of each direct channel of UL UE is used, and a process similar to the step 5 or 6 is used for each DL UE.

In the simulation shown in Figure 2, we examine the performance of the sum rate at UL and DL for two different ranks of the MIMO IBMAC-IC, namely $r = 2$ and $r = 3$. As depicted in Figure 2, the sum rate at UL is almost the same in both cases. This is due to the fact that based on the IA feasibility condition in Theorem 3, it is not possible to increase the DoF at UL UEs (and hence the rate at high SNR) for this system dimension, without violating IA feasibility (Table 2). On the other hand, for the DL side, we can observe in Figure 2 that at high SNR, the sum rate is higher for $r = 2$ compared to $r = 3$, which is also confirmed in the numerical results presented in Table 2. This can be explained by considering a non-uniform DoF at DL UEs (as suggested in Conjecture 1), which enables us to increase the sum rate at high SNR.

Figure 3 illustrates the impact of UE-to-UE interference on the performance of the DynTDD system, where we compare the simulations with two different initialisation: init (UE2UE ZF + BS2UE ZF) and init (UE EigR + BS2UE ZF). The simulation results clearly show that incorporating ZF decoders $\boldsymbol{F}_{z,k}$ and precoders $\boldsymbol{G}_{z,l}$ to mitigate the UE-to-UE interference leads to a significant improvement in the sum rate of the system. In other words, the proposed approach successfully addresses the issue of UE-to-UE interference and enhances the overall performance of the DynTDD system.

Figure 4 presents a comparison of the average sum rate vs. SNR for four different simulations: init (UE2UE ZF + BS2UE ZF), init (UE2UE ZF + BS2UE ZF+ WF), init (UE2UE ZF + BS2UE ZF)+ WMMSE, iter=n and init (UE2UE ZF + BS2UE ZF+ WF)+ WMMSE, iter=n, to evaluate the water-filling algorithm. The simulation results show the sum rate at initialisation and the sum rate at different iterations (1st, 3rd, 10th, and 50th) of the WMMSE algorithm, indicating the convergence behaviour of the algorithm. The comparison also shows that the WMMSE algorithm outperforms the ZF solution at low SNR, but the water-filling algorithm combined with the ZF can approach the performance of the WMMSE algorithm at low SNR.

Figure 2 Sum rate performance with $N_{ul} = 3$, $N_{dl} = 6$, $K_{ul} = 2$ and $K_{dl} = 4$ (see online version for colours)

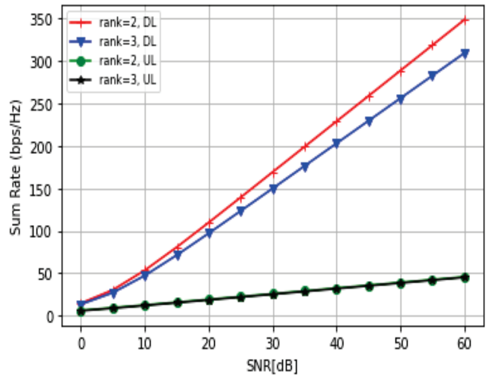

Figure 3 sum rate performance with $N_{ul} = 3$, $N_{dl} = 6$, $K_{ul} = 2$, $K_{dl} = 4$ and $r = 2$ (see online version for colours)

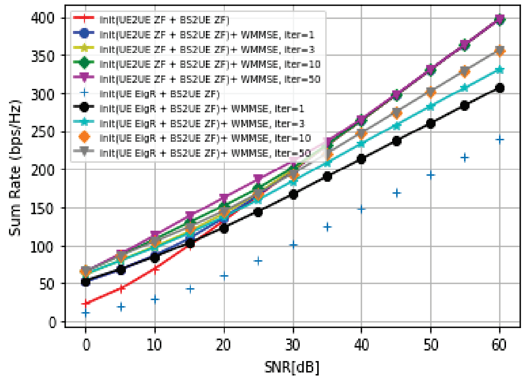

Figure 4 Sum rate performance with $N_{ul} = 3$, $N_{dl} = 6$, $K_{ul} = 2$, $K_{dl} = 4$ and $r = 2$ (see online version for colours)

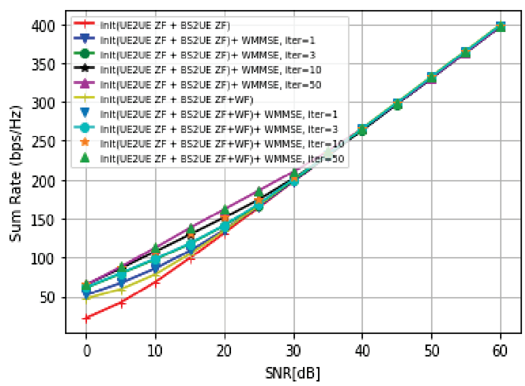

7 Conclusions

In this paper, we present novel findings regarding the feasibility of Interference Alignment (IA) and the potential benefits of non-uniform DoF at DL and/or UL UE in terms of sum DoF maximisation and rate at high SNR. We also compare the evaluation of the sufficient condition in Theorem 4 with the state-of-the-art condition to highlight the achieved improvement.

The focus of this paper is on beamforming design for MIMO IBMAC-IC in DynTDD systems, with the objective of maximising the weighted sum rate. We provide detailed steps to construct ZF beamformers for both DL and UL UEs to cancel all UL-to-DL interference links. Moreover, we consider a ZF transmitter at the DL BS to mitigate intracell interference. In our simulations, we use these ZF filters during initialisation, and then we apply the WMMSE iterative algorithm to maximise the sum rate, which is a potential candidate for practical low-complexity transmit beamforming implementations. We also investigate the impact of the water-filling algorithm during initialisation and how it can improve performance at low SNR. Our numerical results demonstrate that UE-to-UE interference in DynTDD systems can be detrimental to the system's performance, but can also be mitigated by interference alignment techniques.

References

Chen, Y., Huang, Y., Shi, Y., Hou, Y.T., Lou, W. and Kompella, S. (2020) 'On dof-based interference cancellation under general channel rank conditions', *IEEE/ACM Transactions on Networking*, Vol. 28, No. 3, pp.1002–1016.

Christensen, S.S., Agarwal, R., De Carvalho, E. and Cioffi, J.M. (2008) 'Weighted sum-rate maximization using weighted mmse for mimo-bc beamforming design', *IEEE Transactions on Wireless Communications*, Vol. 7, No. 12, pp.4792–4799.

Goldsmith, A. (2005) *Wireless Communications*, Cambridge University Press.

González, Ó., Beltrán, C. and Santamaría, I. (2014) 'A feasibility test for linear interference alignment in mimo channels with constant coefficients', *IEEE Transactions on Information Theory*, Vol. 60, No. 3, pp.1840–1856.

Han, Y., Chang, Y., Cui, J. and Yang, D. (2010), A novel inter-cell interference coordination scheme based on dynamic resource allocation in LTE-TDD systems', *2010 IEEE 71st Vehicular Technology Conference*, 16–19 May, 2010, IEEE, Taipei, Taiwan, pp.1–5.

Jayasinghe, P., Tölli, A. and Latva-aho, M. (2015) 'Bi-directional signaling strategies for dynamic tdd networks', *2015 IEEE 16th International Workshop on Signal Processing Advances in Wireless Communications (SPAWC)*, 27 June – 1 July, 2015, IEEE, Stockholm, Sweden, pp.540–544.

Jeon, S.-W., Kim, K., Yang, J. and Kim, D.K. (2017) 'The feasibility of interference alignment for mimo interfering broadcast-multiple-access channels', *IEEE Transactions on Wireless Communications*, Vol. 16, No. 7, pp.4614–4625.

Ko, K.S., Jung, B.C. and Hoh, M. (2018) 'Distributed interference alignment for multi-antenna cellular networks with dynamic time division duplex', *IEEE Communications Letters*, Vol. 22, No. 4, pp.792–795.

Liu, T. and Yang, C. (2013) 'On the feasibility of linear interference alignment for mimo interference broadcast channels with constant coefficients', *IEEE Transactions on Signal Processing*, Vol. 61, No. 9, pp.2178–2191.

Negro, F., Shenoy, S.P., Ghauri, I. and Slock, D.T. (2010) 'Interference alignment feasibility in constant coefficient mimo interference channels', *2010 IEEE 11th International Workshop on Signal Processing Advances in Wireless Communications (SPAWC)*, 20–23 June, 2010, IEEE, Marrakech, Morocco, pp.1–5.

Negro, F., Shenoy, S.P., Slock, D.T. and Ghauri, I. (2009) 'Interference alignment limits for k-user frequency-flat mimo interference channels', *2009 17th European Signal Processing Conference*, 24–28 August, 2009, IEEE, Glasgow, Scotland, pp.2445–2449.

Rachad, J., Nasri, R. and Decreusefond, L. (2018), Interference analysis in dynamic tdd system combined or not with cell clustering scheme', *2018 IEEE 87th Vehicular Technology Conference (VTC Spring)*, 3–6 June, 2018, IEEE, Porto, Portugal, pp.1–5.

Razaviyayn, M., Lyubeznik, G. and Luo, Z.-Q. (2011) 'On the degrees of freedom achievable through interference alignment in a mimo interference channel', *IEEE Transactions on Signal Processing*, Vol. 60, No. 2, pp.812–821.

Shi, Q., Razaviyayn, M., Luo, Z.-Q. and He, C. (2011) 'An iteratively weighted mmse approach to distributed sum-utility maximization for a mimo interfering broadcast channel', *IEEE Transactions on Signal Processing*, Vol. 59, No. 9, pp.4331–4340.

Tibhirt, A., Slock, D. and Yuan-Wu, Y. (2021), Distributed beamforming design in reduced-rank mimo interference channels and application to dynamic tdd', *WSA 2021; 25th International ITG Workshop on Smart Antennas*, VDE, pp.1–6.

Tibhirt, A., Slock, D. and Yuan-Wu, Y. (2022a) 'Interference alignment in reduced-rank mimo networks with application to dynamic tdd', *2022 20th International Symposium on Modeling and Optimization in Mobile, Ad hoc, and Wireless Networks (WiOpt)*, 19–22 September, 2022, IEEE, Turin, Italy, pp.338–344.

Tibhirt, A., Slock, D. and Yuan-Wu, Y. (2022b) 'Interference mitigation in dynamic tdd mimo interference channels', *2022 IEEE 27th International Workshop on Computer Aided Modeling and Design of Communication Links and Networks (CAMAD)*, 2–3 November, 2022, IEEE, Paris, France, pp.7–12.

Yang, H.H., Geraci, G., Zhong, Y. and Quek, T.Q. (2017) 'Packet throughput analysis of static and dynamic tdd in small cell networks', *IEEE Wireless Communications Letters*, Vol. 6, No. 6, pp.742–745.

Note

[1]This distribution of singular values is used to dedicate the first effective antennas to the reception/transmission of the useful signal.